Curvature-Dependent Elastic Properties of Liquid-Ordered Domains Result in Inverted Domain Sorting on Uniaxially Compressed Vesicles

H. Jelger Risselada,[1,*] Siewert Jan Marrink,[2] and Marcus Müller[3]

[1]*Theoretical Molecular Biophysics Group, Max-Planck-Institute for Biophysical Chemistry, 37077 Göttingen, Germany*
[2]*University of Groningen, Nijenborgh 4, 9747 AG Groningen, The Netherlands*
[3]*Institut für Theoretische Physik, Georg-August-Universität, 37077 Göttingen, Germany*

(Received 21 October 2010; published 5 April 2011; publisher error corrected 7 April 2011)

Using a coarse-grained molecular model we study the spatial distribution of lipid domains on a 20-nm-sized vesicle. The lipid mixture laterally phase separates into a raftlike, liquid-ordered (l_o) phase and a liquid-disordered phase. As we uniaxially compress the mixed vesicle keeping the enclosed volume constant, we impart tension onto the membrane. The vesicle adopts a barrel shape, which is composed of two flat contact zones and a curved edge. The l_o domain, which exhibits a higher bending rigidity, segregates to the highly curved edge. This inverted domain sorting switches to normal domain sorting, where the l_o domain prefers the flat contact zone, when we release the contents of the vesicle. We rationalize this domain sorting by a pronounced reduction of the bending rigidity and area compressibility of the l_o phase upon bending.

DOI: 10.1103/PhysRevLett.106.148102 PACS numbers: 87.14.Cc

Lipids and proteins are not homogeneously distributed in the cell membrane [1] and much effort has been directed towards understanding how intracellular trafficking maintains the composition differences between the various membrane compartments of the cell. Without proteins or alternative, active sorting mechanisms, the interplay between local membrane curvature and lipid shape dictates the spatial distribution of lipids. Curvature-induced lipid sorting has attracted abiding interest by theory [2–5] and experiment [6,7]. The free-energy reduction of curvature-induced lipid sorting is weak, and it is insufficient to overcome the entropy of mixing in an ideal mixture of lipids. The cooperative behavior of lipid mixtures in the vicinity of the demixing transition or in the laterally phase-separated state, however, amplifies the effect. Curvature may induce sorting of phase-separated lipid domains, and the concomitant line tension between domains may also alter the membrane topology (e.g., budding [8]). Indeed, experiments of laterally phase-separated mixed vesicles have observed that domains with a larger resistance toward bending segregate to less curved membrane regions while domains with a lower bending rigidity enrich at highly curved areas [6,7]. The total free-energy gain for this ''normal'' domain sorting due to the different bending rigidities of domains is on the order of the bending rigidity contrast between the domains and independent of the size of the vesicle.

In this Letter we present evidence that a contrast of the curvature dependence of the elastic properties of the lipid domains yields an important additional contribution to the free energy of a mixed vesicle under tension. This curvature dependence introduces a fourth-order bending energy and a coupling between the curvature and area compressibility, which can outweigh the contribution of the bending rigidity and result in an ''inverted'' domain sorting; i.e., the domain with the larger bending rigidity segregates to the curved portion of the vesicle. Such a curvature dependence of the elastic membrane properties naturally arises from the change of the internal membrane structure upon bending.

We study the behavior of uniaxially compressed, small vesicles by coarse-grained (CG) molecular dynamics simulations and rationalize the observations by a simple analytical model based on a modified curvature-elasticity Hamiltonian. We describe a mixture of a saturated lipid (dipalmitoyl-phosphatidylcholine, diC_{16}-PC), a polyunsaturated lipid (dilinoleyl-phosphatidylcholine, $diC_{18:2}$-PC), and cholesterol with a global composition ratio, diC_{16}-PC:$diC_{18:2}$-PC:cholesterol = 0.42:0.28:0.3 within the MARTINI force field [9]. This CG model retains most of the structural properties of the lipid molecules on the atomistic scale and simultaneously allows us to address the time and length scales involved in the collective phenomena of lipid domain sorting. At high temperature, $T = 323$ K, the ternary mixture does not laterally phase separate. The ternary mixture at low temperature, $T = 295$ K, however, is strongly segregated into a raftlike, liquid-ordered (l_o) domain that is almost a pure binary mixture of saturated lipid and cholesterol (diC_{16}-PC:$diC_{18:2}$-PC:cholesterol = 0.61:0.01:0.37) and a liquid-disordered (l_d) phase with composition diC_{16}-PC:$diC_{18:2}$-PC:cholesterol = 0.08:0.75:0.17 [10]. The area fraction of the raftlike, l_o domain is $\bar{\varphi}_0 \approx 0.64$ on a tension-free vesicle. The properties of the coexisting domains have been previously characterized [10].

We consider domain sorting on a uniaxially compressed vesicle of diameter $D = 2R_0 = 20$ nm. Initially, the shape of the tension-free vesicle is spherical and, subsequently,

it is uniaxially compressed together with its own periodic image. Compression gives rise to a barrel-shape deformation of the vesicle; i.e., the vesicle is composed of a flat contact zone and a highly curved rim as illustrated in Figs. 1(a) and 1(b). The curvature radius of the rim, $R \approx 6$ nm, compares to the high curvature region in the experimental setup, where a lipid nanotube (10–100 nm radii) is pulled out of a micrometer-sized vesicle, and lipids can free exchange between these two regions with markedly different curvatures [6,7]. In contrast to the experimental setup, however, the conservation of the enclosed volume of the squeezed vesicle in our simulation imparts a significant tension onto the membrane as its shape deviates from the spherical one.

The compression of the mixed vesicle is performed at elevated temperature, $T = 323$ K, in the one-phase region of the ternary mixture. The time evolution of the composition in the flat contact zone is presented in Fig. 1(c).

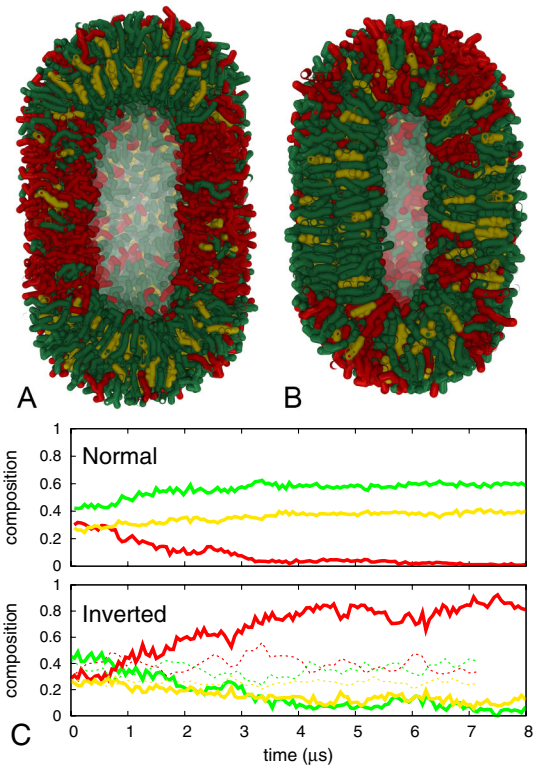

FIG. 1 (color online). Curvature-mediated domain sorting ($T < T_c$, 295 K). (a) Inverted domain sorting in the compressed vesicle after 4 μs ($R = 6$ nm, $\Delta p \approx 95$ bar). (b) Removal of 40% internal solvent recovers normal sorting ($R = 6$ nm, $\Delta p = 0$ bar). (c) Time evolution of the membrane composition in the flat contact zone for normal (upper panel) and inverted domain sorting (lower panel). In the case of inverted sorting (lower panel), the concentration of unsaturated $diC_{18:2}$-PC (red lines) increases, while the concentration of l_o-phase forming components, diC_{16}-PC (green lines) and cholesterol (yellow lines), decreases. The thin dotted lines represent the negative control simulation at 323 K ($T > T_c$). In the case of normal sorting (upper panel), the effect is reversed, and the expected depletion of unsaturated $diC_{18:2}$-PC (red line) is observed.

In accord with previous studies, no indication of lipid sorting is observed in a simulation run of 7 μs duration. Thus, the simulation results of our CG model corroborate that curvature-driven sorting requires collective lipid behavior in the vicinity of demixing or in the phase-separated state.

If domain sorting of the ternary, phase-separated mixture were purely dictated by the contrast of the bending rigidity of the coexisting domains, we would expect that the rigid l_o phase prefers the flat contact zone and the more flexible l_d phase the highly curved rim. Indeed at 295 K we do observe definite, curvature-driven sorting of lipid domains in our simulations, but, contrary to expectation and experiments with membrane tubes, the rigid l_o domain is located at the curved rim while the more flexible l_d domain is located at the flat contact zone. This inverted sorting of lipid domains is clearly visible in the snapshot presented in Fig. 1(a).

In Fig. 1(c) we depict the time evolution of the composition in the flat contact zone after quenching the vesicle into the miscibility gap, $T = 323$ K $\rightarrow$ 295 K. On the time scale of 4 μs, we observe that the flat contact zone becomes gradually enriched with the unsaturated lipid.

Intriguingly, when we lower the surface tension Σ of the squeezed vesicle toward the approximately tension-free state by removing 40% of the enclosed internal solvent, while simultaneously keeping the level of compression R constant, we observe that the curvature preference of the liquid phases switches and normal domain sorting is recovered, i.e., the l_o phase segregates into the flat membrane region as shown in Figs. 1(b) and 1(c).

A potential explanation for the inverted ordering would be a preferential attraction of l_d domains to the contact zone of the compressed vesicle. When we compress the vesicle with its own periodic image, the lipid headgroups in the two flat contact regions become partly dehydrated. To discern whether this effect drives the inverted curvature sorting, we additionally compressed the vesicle between two purely repulsive parallel planes that only interacted with the hydrophobic groups of the lipids. The latter technique allows full hydration of the polar headgroups under compression [11]. However, the same inverted domain sorting was observed even when hydration was maintained.

In order to rationalize the domain sorting we resort to a simple, phenomenological description in terms of a modified Canham-Helfrich Hamiltonian [12,13], which includes the curvature dependence of the elastic properties of the l_o domain. The free energy of a mixed vesicle is composed of a bending and stretching contribution, as well as a contribution due to the line tension λ between the two domains. One obtains the shape of the vesicle and distribution of lipids by minimizing the free energy constraining the total number of lipids in both domains, the enclosed volume, and the distance between the two flat contact zones.

To make progress, we assume that the geometry of the vesicle is barrel shaped, as illustrated in the inset of Fig. 2. This approximate shape is characterized by the radius ρ of

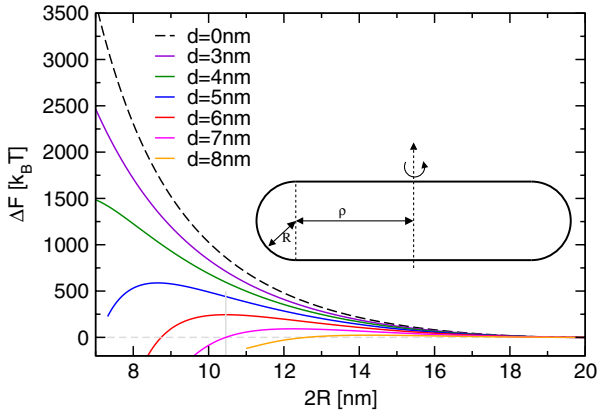

FIG. 2 (color online). Difference of free energy ΔF between inverted and normal domain sorting as a function of the distance $2R$ between the flat contact zones of the vesicle and different values of the curvature dependence d as indicated in the key. The size of the noncompressed vesicle is $2R_0 = 20$ nm. The inset depicts the barrel-shape geometry with half the thickness R and radius of the contact zone ρ.

the flat contact zone and the radius R of the curved rim. The volume and surface area of the vesicle are given by the approximate expressions $V \approx \frac{4\pi}{3}R^3 + \pi^2R^2\rho + 2\pi R\rho^2$ and $S \approx 4\pi R^2 + 2\pi^2 R\rho + 2\pi\rho^2$, respectively. The mean curvature of the rim is $H \approx \frac{1}{2}(\frac{1}{R} + \frac{1}{R+(\pi/2)\rho})$, and we neglect the contribution of the Gaussian curvature in the following. Values of the Gaussian bending rigidity of our systems are not precisely known, and we do not expect this approximation to qualitatively alter the results.

We also ignore the line-tension contribution. This effect leads to budding of minority domains from planar membranes provided that the lateral extent of the domain is larger than the invagination length, κ_b/λ with κ_b being the bending rigidity [8]. It limits the size of lateral domains on membranes adsorbed to periodically corrugated substrates [5], or leads to multiple, stable domains on vesicles [14]. In our simulation, however, the l_o domain is the majority component. Moreover, using the values $\kappa_{b,l_o,0} \approx 4 \times 10^{-19}$ J [15] and $\lambda \approx 3.5$ pN [10], we find that the concomitant length scale, $\kappa_b/\lambda = 114$ nm, exceeds the vesicle size R_0. Additionally, line-tension effects cannot explain why domain sorting switches from inverted to normal as we reduce the enclosed volume without altering membrane composition or vesicle geometry.

The density of the two apposing monolayers is not individually considered, which would lead to a difference-area contribution to the free energy upon bending [16]. The fast flip-flop of cholesterol in the liquid-disordered phase [17] and the exchange of cholesterol between the domains partially mitigates this effect. With these assumptions the free energy of the vesicle takes the form

$$\begin{aligned}\Phi[\bar{\varphi}, \tilde{\sigma}_{l_o}, \tilde{\sigma}_{l_d}, \tilde{\sigma}'_{l_d}, \rho, R] = {} & \frac{\kappa_{b,l_o}(H)}{2}\bar{\varphi}S[2H]^2 + \frac{\kappa_{b,l_d}(H)}{2}([1-\bar{\varphi}]S - 2\pi\rho^2)[2H]^2 + \frac{\kappa_{a,l_o}(H)}{2}\bar{\varphi}S[\tilde{\sigma}_{l_o} - 1]^2 \\ & + \frac{\kappa_{a,l_d}(H)}{2}([1-\bar{\varphi}]S - 2\pi\rho^2)[\tilde{\sigma}_{l_d} - 1]^2 + \frac{\kappa_{a,l_d}(0)}{2}2\pi\rho^2[\tilde{\sigma}'_{l_d} - 1]^2 + \Sigma_{l_o}[\bar{\varphi}S\tilde{\sigma}_{l_o} - \bar{\varphi}_0 S_0] \\ & + \Sigma_{l_d}\{([1-\bar{\varphi}]S - 2\pi\rho^2)\tilde{\sigma}_{l_d} + 2\pi\rho^2\tilde{\sigma}'_{l_d} - (1-\bar{\varphi}_0)S_0\} - p(V - V_0) - F(2R - D), \end{aligned} \quad (1)$$

where κ_{b,l_o}, κ_{a,l_o} and κ_{b,l_d}, κ_{a,l_d} are the bending rigidity and area compressibilities of the two domains. $\tilde{\sigma}_{l_o}$, $\tilde{\sigma}_{l_d}$, $\tilde{\sigma}'_{l_d}$ denote the normalized lipid densities in the l_o domains on the rim and of the l_d domain on the rim and on the flat contact zone, respectively. The area fraction of the l_o domain is termed $\bar{\varphi}$. Σ_{l_o}, Σ_{l_d}, p, and F are Lagrange multipliers that enforce the total number of lipids in the l_o and l_d domains, the enclosed volume, and the distance of the contact zones. The combination of the quadratic increase of the free energy with deviations of the normalized lipid density from its reference value and the constraint of the total number of lipids constitutes the free energy of stretching a vesicle.

In the molecular simulations we observe that the thickness of the l_o and l_d domains upon squeezing decreases by approximately 15% [4.6(1) nm $\rightarrow$ 4.0(1) nm] and 8% [3.8(1) nm $\rightarrow$ 3.5(1) nm], respectively. We estimated the area compressibility of l_o and l_d phase from the simulated stress-strain relation using a 10×10 nm^2 bilayer patch with corresponding composition and obtained, $\kappa_{a,l_o,0} = 1200$ mN/m $= 290 k_B T/\text{nm}^2$ and $\kappa_{a,l_d,0} = 200$ mN/m $= 48 k_B T/\text{nm}^2$, in agreement with experimentally reported values [18,19]. Assuming that the shrinking of the thickness is compensated by a lateral stretching, $\Delta S = S - S_0$, we would estimate the tension Σ in the l_o domain to be $\Sigma = \kappa_{a,l_o,0}\Delta S/S_0 = 180$ mN/m, while the value in the l_d domain would be $\Sigma = 16$ mN/m. This estimate violates the mechanical equilibrium between the domains, and the tension in the l_o domain also is about twice as large as the one measured in the simulation, $\Sigma = 57(5)$ mN/m, via three-dimensional pressure field [20]. Thus, the elastic constants of the domains are affected by changes of curvature or tension that result from squeezing the vesicle. When we simulated the corresponding but flat l_o bilayer patch under similar tension ($\Sigma = 60$ mN/m), the decrease in thickness was only 5% [4.4(1) nm] being about 3 times smaller than for the curved l_o phase. This *additional* thinning of the l_o phase under curvature stems from the distortion in lipid-tail ordering, which results from the asymmetric packing geometry in the curved bilayer [21] and effectively softens the l_o phase. Moreover, the curved l_o phase exhibits an asymmetric composition between the

two apposing leaflets. For the curved l_o phase we obtained a cholesterol content of 39% for the inner and 26% for the outer leaflet. This difference stems from the ability of cholesterol to redistribute itself across the bilayer (flip-flop) and its intrinsic negative curvature [22] favoring the inner leaflet over the outer leaflet.

These pronounced structural changes of the l_o domain upon bending are modeled by curvature-dependent elastic properties, $\kappa_{b,l_o} = \kappa_{b,l_o,0}(1 - [d_b H]^2)$ and $\kappa_{a,l_o} = \kappa_{a,l_o,0}(1 - [d_a H]^2)$, where d_a and d_b are constants with dimension length. This dependence can be conceived as, first, additional terms of a systematic expansion of the elastic properties with respect to curvature around the reference state of a flat, symmetric bilayer. As such, a dependence does not depend on the sign of curvature, the linear term vanishes. The introduction of curvature-dependent elastic properties is completely equivalent to augmenting the Helfrich Hamiltonian by a fourth-order bending contribution and a coupling between the square of the curvature and area compressibility. It remains to be investigated if this augmented Helfrich Hamiltonian provides a quantitatively accurate description of the highly curved vesicles considered in the simulation. The two additional terms, however, are the minimal ingredients required to rationalize the observation. d_a and d_b are expected to be on the order of the bilayer thickness, and we take $d \equiv d_b = d_a$. The dependence of all other material constants on curvature is neglected.

We minimize the free energy, Eq. (1), of the vesicle with respect to the parameter $\bar{\varphi}$, $\tilde{\sigma}_{l_o}$, $\tilde{\sigma}_{l_d}$, and $\tilde{\sigma}'_{l_d}$, and fulfill the constraints. The numerical calculations use the values $\kappa_{b,l_o} = 100 k_B T$, $\kappa_{b,l_d} = 15 k_B T$, $\kappa_{a,l_o,0} = 290 k_B T/\mathrm{nm}^2$, and $\kappa_{a,l_d,0} = 48 k_B T/\mathrm{nm}^2$, and the strength of the curvature dependence is varied $0 \le d \le 8$ nm.

The results for the free-energy difference ΔF between inverted and normal domain sorting are depicted in Fig. 2. For $d = 7$ nm, we find that reverse sorting occurs for $2R < 10.46$ nm. At this point, $H \approx 0.126\ \mathrm{nm}^{-1}$, and the elastic constants of the l_o domain are reduced by a factor $(1 - [dH]^2) \approx 0.222$, but the l_o domain remains stiffer and less compressible than the l_d domain. Moreover, while the overall surface increases by about 11.2%, the area of the l_o domain increases by only 9.6% because it is less stretchable. The calculations also show that deflating the vesicle shifts the onset of inverted ordering to larger values of the curvature.

The scale separation between the forces that determine the geometric shape of the vesicle and the forces that dictate the placement of the domains allows us to qualitatively discuss the two counteracting effects. (I) The different bending rigidities favor the l_d domain be located on the curved rim. The concomitant free-energy difference of inverted domain sorting scales like $\Delta F_{\mathrm{bend}} \sim 4\pi[(\kappa_{b,l_d} - \kappa_{b,l_o})]$ and is independent from the vesicle size. Assuming the values for a planar bilayer, this free-energy difference is $\Delta F_{\mathrm{bend}} \sim 1068 k_B T$. Including the curvature dependence, our model predicts the free-energy difference remains positive but is significantly reduced, i.e., $\Delta F_{\mathrm{bend}} \sim 89 k_B T$ for $H = 0.126\ \mathrm{nm}^{-1}$ and $d = 7$ nm. (II) Placing the l_o domain on the curved part of the membrane surface instead of the flat portion will reduce the free energy by an amount of the order $\Delta F_{\mathrm{stretch}} \sim -\frac{\kappa_{a,l_o,0}}{2}(dH)^2(\frac{\Delta S_{l_o}}{S_{l_o}})^2 S \sim -1900 k_B T$ for $\frac{\Delta S^{l_o}}{S^{l_o}} = 0.11$, which outweighs the bending contribution for highly compressed vesicles.

Thus the Canham-Helfrich model augmented by a curvature dependence of the elastic properties is able to rationalize the effect observed in the simulations semi-quantitatively. We propose that the effect discussed here might be experimentally obtained by compression of nanometer-sized vesicles between, e.g., two glass plates. In this case, the difference in both orientation and position of the liquid phases with respect to the glass plates likely allows determination of the inverted domain sorting. Additional details of our simulations and elasticity model can be found in the supplemental material [23].

We thank H. Grubmüller, R. Lipowsky, and I. Szleifer for critically reading the manuscript. Financial support by the DFG under Grants No. SFB 803/B2 and B3 is gratefully acknowledged.

*hrissel@gwdg.de

[1] G. van Meer *et al.*, Nat. Rev. Mol. Cell Biol. **9**, 112 (2008).
[2] U. Seifert, Phys. Rev. Lett. **70**, 1335 (1993).
[3] V. Kralj-Iglic *et al.*, J. Phys. A **35**, 1533 (2002).
[4] I. R. Cooke and M. Deserno, Biophys. J. **91**, 487 (2006).
[5] B. Rozycki, T. R. Weikl, and R. Lipowsky, Phys. Rev. Lett. **100**, 098103 (2008).
[6] B. Sorre *et al.*, Proc. Natl. Acad. Sci. U.S.A. **106**, 5622 (2009).
[7] M. Heinrich *et al.*, Proc. Natl. Acad. Sci. U.S.A. **107**, 7208 (2010).
[8] R. Lipowsky, J. Phys. II (France) **2**, 1825 (1992).
[9] S. J. Marrink *et al.*, J. Phys. Chem. B **111**, 7812 (2007).
[10] H. J. Risselada and S. J. Marrink, Proc. Natl. Acad. Sci. U.S.A. **105**, 17 367 (2008).
[11] H. J. Risselada *et al.*, J. Phys. Chem. B **112**, 7438 (2008).
[12] P. B. Canham, J. Theor. Biol. **26**, 61 (1970).
[13] W. Helfrich, Z. Naturforsch. C **28**, 693 (1973).
[14] E. Gutlederer *et al.*, Soft Matter **5**, 3303 (2009).
[15] R. S. Gracia *et al.*, Soft Matter **6**, 1472 (2010).
[16] U. Seifert, Adv. Phys. **46**, 13 (1997).
[17] S. J. Marrink *et al.*, J. Am. Chem. Soc. **131**, 12 714 (2009).
[18] K. J. Tierney *et al.*, Biophys. J. **89**, 2481 (2005).
[19] D. Needham and S. N. Rashmi, Biophys. J. **58**, 997 (1990).
[20] O. H. Ollila *et al.*, Phys. Rev. Lett. **102**, 078101 (2009).
[21] H. J. Risselada and S. J. Marrink, Phys. Chem. Chem. Phys. **11**, 2056 (2009).
[22] W. Wang *et al.*, Biophys. J. **92**, 2819 (2007).
[23] See supplemental material at http://link.aps.org/supplemental/10.1103/PhysRevLett.106.148102 for details of our simulations and elasticity model.